

C.52



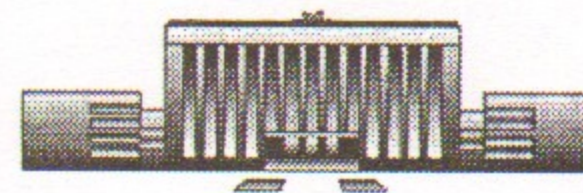
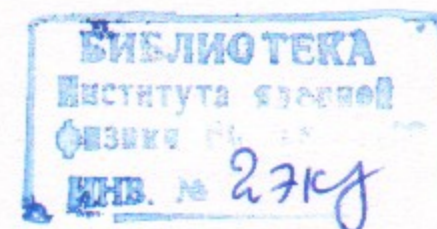
Siberian Branch of Russian Academy of Science  
BUDKER INSTITUTE OF NUCLEAR PHYSICS

B.V. Chirikov and V.G. Davidovsky

THE STRUCTURE  
OF CHAOTIC ATTRACTOR  
IN A FEW-FREEDOM DYNAMICAL SYSTEM

Budker INP 99-96

<http://www.inp.nsk.su/publications>



Novosibirsk  
1999

✓

# The structure of chaotic attractor in a few-freedom dynamical system

*B.V. Chirikov and V.G. Davidovsky*

Budker Institute of Nuclear Physics  
630090 Novosibirsk, Russia

## Abstract

The results of numerical experiments on the structure of chaotic attractors in the Khalatnikov - Kroyter model of two freedoms are presented. The attractor dimension, size, and the maximal Lyapunov exponent in dependence on the single dimensionless parameter  $F$  of the model are found and discussed. We were able to discern four different attractors characterized by a specific critical value of the parameter ( $F = F_{cr}$ ), such that the attractor exists for  $F > F_{cr}$  only. A simple empirical relation for this dependence on the argument ( $F - F_{cr}$ ) is presented which turns out to be universal for different attractors with respect to the dimension and dimensionless Lyapunov exponents. Yet, it differs as to the size of attractor. In the main region of our studies the dependence of all dimensionless characteristics of the chaotic attractor on the parameter  $F$  is very slow (logarithmic) which is qualitatively different as compared to that of a multi-freedom attractor, e.g., in turbulence (a power law). However, preliminary numerical experiments at very large  $F \sim 10^7$  indicate a transition to a power-law dependence in a few-freedom system as well.

Email: [chirikov@inp.nsk.su](mailto:chirikov@inp.nsk.su)

©Budker Institute of Nuclear Physics SB RAS

## 1 Introduction

In the present paper we continue numerical experiments [1] with the Khalatnikov - Kroyter model [2] developed for a qualitative description of the wave turbulence of second sound in helium.

The model is specified by an effective non-Hermitian Hamiltonian:

$$H(a_1, a_2) = (\omega_1 - i\gamma_1)|a_1|^2 + (\omega_2 - i\gamma_2)|a_2|^2 + (\mu a_1^2 a_2^* + f a_1^* + \text{c.c.}) \quad (1.1)$$

where we slightly changed the notations in Ref. [2, 1]. This Hamiltonian describes the two linear oscillators via complex phase-space variables  $a_j$  ( $j = 1, 2$ ) and the frequencies  $\omega_j - i\gamma_j$  with phenomenological dissipation parameters  $\gamma_j$ . Two other parameters of the model represent a nonlinear coupling  $\mu$  of the two oscillators, and the driving force  $f$ .

The motion equations

$$\begin{aligned} i\dot{a}_1 &= (\omega_1 - i\gamma_1)a_1 + 2\mu a_1^* a_2 + f \\ i\dot{a}_2 &= (\omega_2 - i\gamma_2)a_2 + \mu a_1^2 \end{aligned} \quad (1.2)$$

were numerically integrated together with the corresponding linearized equations (for details see Ref. [1]). Particularly, all four Lyapunov exponents ( $\lambda_1 \geq \lambda_2 \geq \lambda_3 \geq \lambda_4$ ) were computed. One of them, whose eigenvector goes along the trajectory, is always zero while the sum of all

$$\lambda_\Gamma = \sum_{n=1}^4 \lambda_n = -2(\gamma_1 + \gamma_2) = \text{const} \quad (1.3)$$

is the constant rate of the phase space volume contraction.

Surprisingly, at a relatively weak force  $f$  this most simple model does describe the birth of turbulence (dynamical chaos) in a physical system. This was the main subject of studies in Ref. [2, 1].

As the force grows the two-freedom model is losing any relation to the real physical turbulence which is a multi(infinitely)-freedom phenomenon. Nevertheless, it seems of some interest, for the general theory of dynamical systems, to compare the structure and properties of a chaotic attractor in such an opposite limit represented by a simple model under consideration. It was the main motivation for us to continue general studies of the model on unrestricted range of its parameters.

## 2 Scaling

In the spirit of the theory of turbulence we introduce, first, a unique dimensionless parameter, similar to the Reynolds number, which determines all the dimensionless characteristics of the motion. To this end, we choose  $f$ ,  $\mu$ ,  $\gamma$  as the three basic parameters, and form the desired combination

$$F = \frac{f\mu}{\gamma^2} \quad (2.1)$$

which has the meaning of a dimensionless force. For this basic characteristic of the model were unique we need to fix all other dimensionless parameters:

$$\frac{\omega_1}{\omega_2} = 0, \quad \frac{\gamma_1}{\gamma_2} = 0.25, \quad \text{and} \quad \frac{\omega_2}{\gamma_2} = -12.5 \quad (2.2)$$

The values of all three ratios are chosen as in the previous studies [2, 1]. Particularly, we keep  $\omega_1 = 0$ , as well as the motion initial conditions

$$a_1(0) = a_2(0) = 0 \quad (2.3)$$

This allows us to directly compare our new results with the former ones. In what follows we set  $\gamma = \gamma_2$  in the basic relation (2.1).

Invariance of  $F$  with respect to variation of the three basic parameters gives us an extra freedom for choosing the latter in such a way to minimize the computation errors, and thus to reach higher values of  $F$ .

In the present studies we were primarily interested in the properties of chaotic attractor. One of its principal characteristic is the metric ( $M$ ) that is the set of signs of the Lyapunov exponents. As in the previous studies we did observe only one metric of the three possible, namely

$$M = (+, 0, -, -) \quad (2.4)$$

with a single zero exponent  $\lambda_2 = 0$ . The next, more interesting, characteristic of attractor is the fractal (noninteger) dimension. By now, there is a dozen

of various definitions for such a dimension (see, e.g., Ref. [3]). From physical point of view those all are meaningful and acceptable in principle. However, in numerical experiments the two of them are much more preferable. These make use the Lyapunov exponents only which greatly simplifies the computation. We have chosen one, due to Kaplan and Yorke, because it is more close to other definitions [4, 5]. It is given by the relation

$$d = m + \frac{\sum_{n=1}^m \lambda_n}{|\lambda_{m+1}|} \quad (2.5a)$$

where  $m$  is the largest integer for which the sum  $\sum_{n=1}^m \lambda_n \geq 0$ . This is the simplest and widely used method for calculating dimension. In the model under consideration the dimension of a chaotic attractor is always within the interval ( $2 < d < 4$ ). The upper bound corresponds to the dimension of the whole phase space, while the lower is the condition for chaos ( $\lambda_1 > 0$ , see Eq.(2.4)).

The second characteristic of a chaotic attractor, closely related to (but different from) the former is the maximal Lyapunov exponent  $\lambda_1$ . In dimensionless form it is

$$\Lambda_1 = \frac{\lambda_1}{\gamma} \quad (2.5b)$$

Accordingly, the dimensionless sum of all the exponents  $\Lambda_\Gamma = \lambda_\Gamma/\gamma = -2.5$  (see Eq.(1.3)).

Besides, we computed two other, geometrical, characteristics of attractor: the average size and shape. The former is represented by attractor's rms radius in phase space

$$R = \sqrt{R_1^2 + R_2^2}, \quad R_j^2 = \langle A_j^2 \rangle - \langle A_j \rangle^2 \approx \langle A_j^2 \rangle \quad (2.5c)$$

where  $A_j = a_j \sqrt{\mu/f}$  ( $j = 1, 2$ ) are dimensionless variables, and the brackets  $\langle \rangle$  denote the time average along a trajectory. In all cases the average shift of attractors  $\langle A_j \rangle$  was relatively small. The attractor shape is characterized by the ratio

$$S = \frac{R_2}{R_1} \quad (2.5d)$$

The results are presented and discussed in the next Section.

## 3 Results and discussion

In Fig.1 the attractor dimension  $d$ , Eq.(2.5a), is plotted in dependence on the principal parameter  $F$ , Eq.(2.1). The huge range of  $F$  comprises almost

five orders of magnitude, from the first chaos border at  $F = F_{cr} = 173$  up to  $F \approx 10^7$  limited by the computation time (about one full day). Five separated groups of points are clearly seen followed by a number of scattered points. Each group corresponds to a chaos window in  $F$  separated from the neighbours by the limit-cycle windows. Apparently, the latter also exist in the region of scattered points which all belong to chaotic attractors. However, these points are too few, because of computation difficulties, for the reliable location of any windows beyond  $F \sim 10^4$ .

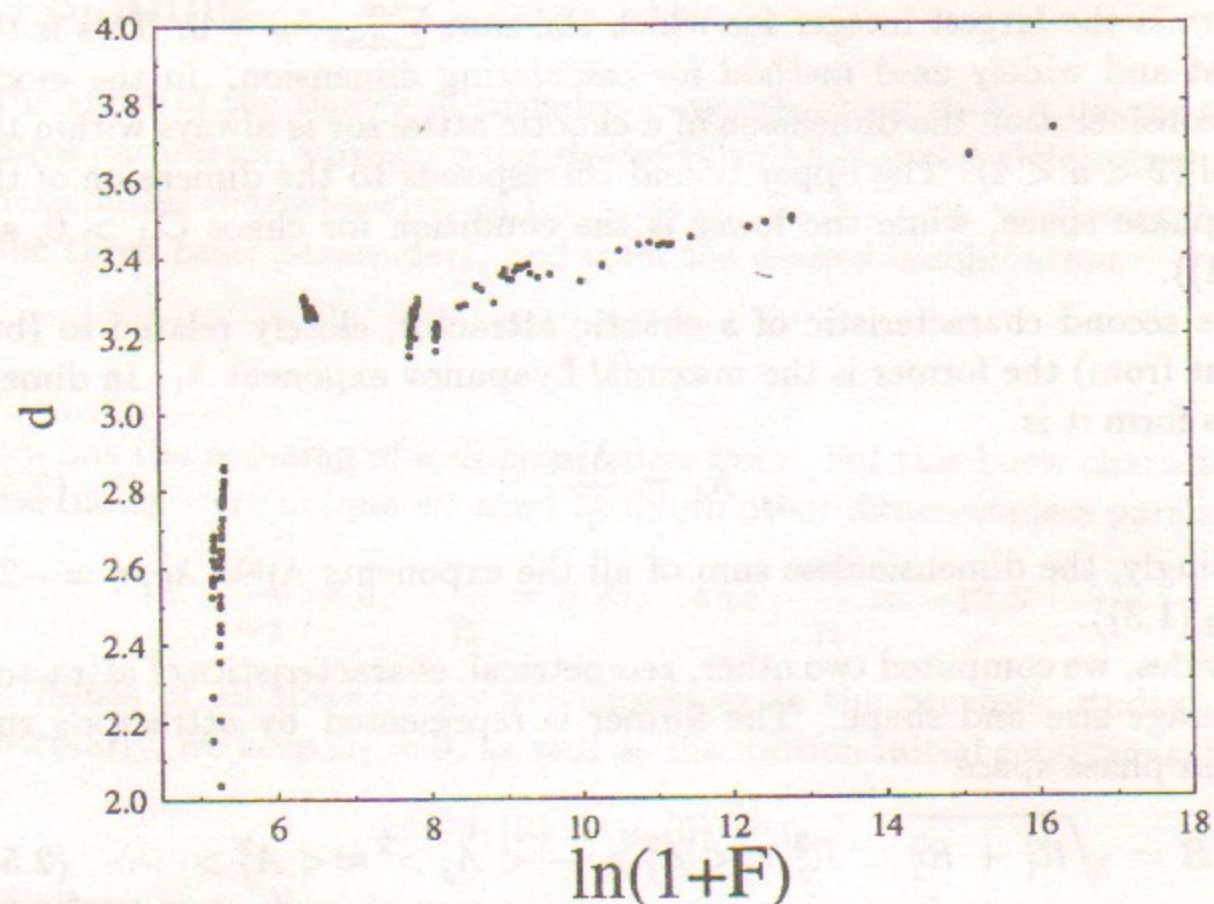


Figure 1: Chaotic attractor dimension vs. principal parameter  $F$  in a semilog scale (see text). Gaps between groups of points correspond to limit-cycle attractors.

The first two groups, studied already in our previous work [1], certainly belong to different attractors with different chaos borders  $F_{cr} \approx 173$  and  $190$ , respectively. It is natural, again in the spirit of the theory of turbulence, to introduce the principal argument of all dependences in the form:

$$\delta F = F - F_{cr} \quad (3.1)$$

where  $F_{cr}$  is the corresponding chaos border which is characteristic, and different, for a particular attractor.

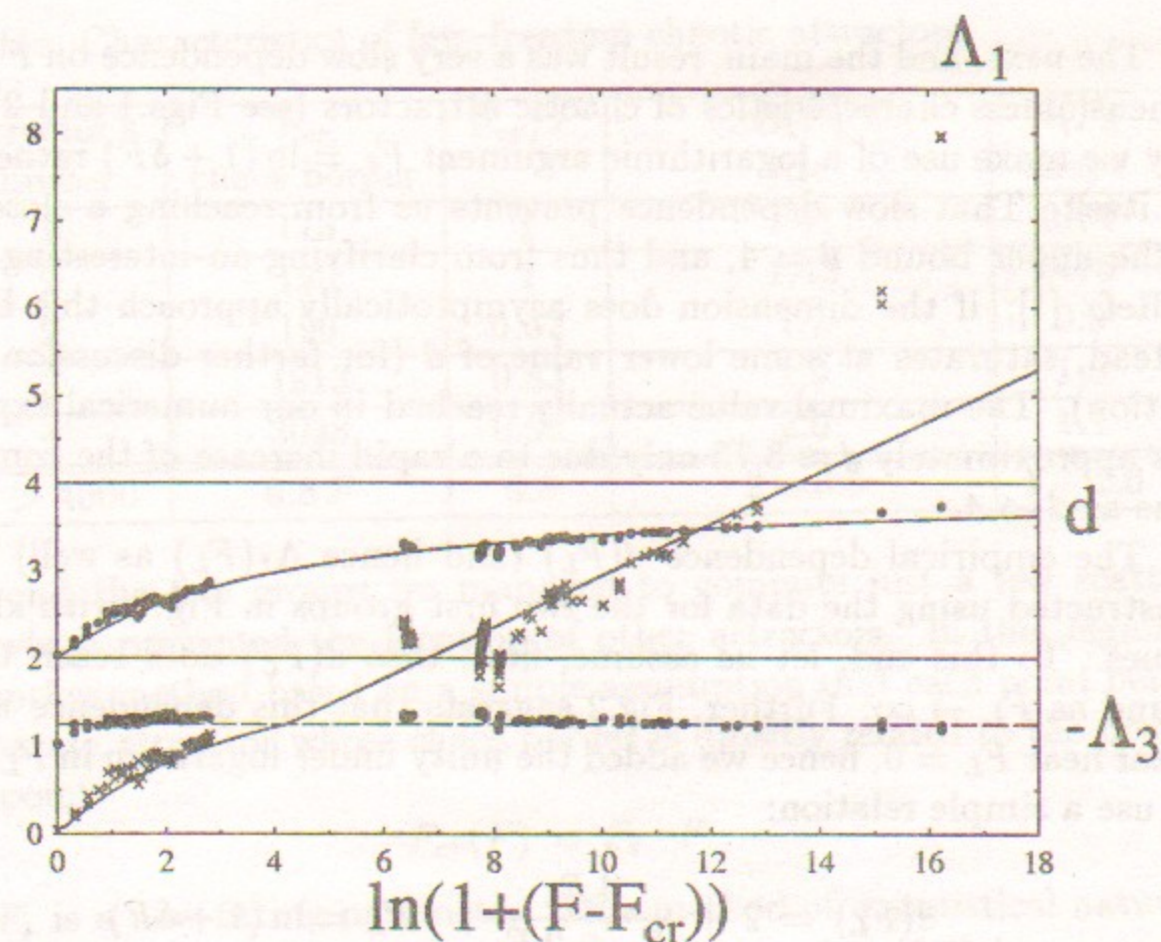


Figure 2: Dependence of the attractor dimension  $d$  (upper points), maximal Lyapunov exponent  $\Lambda_1$  (crosses), and  $-\Lambda_3$  (lower points) on the parameter  $\delta F$  (3.1). In this figure  $F_{cr} = 173$  and  $190$  for the two first groups of points in Fig.1, and  $F_{cr} = 0$  for all other points (cf. Figs.1 and 3). Two solid horizontal lines indicate the dimension interval ( $2 < d < 4$ ). The dashed line is the mean  $\langle -\Lambda_3 \rangle \approx 1.25$ . Two curves are empirical relations (3.3) and (3.2) for  $d$  and  $\Lambda_1$ , respectively;  $F_0 = 8.5$ .

The result of such a rescaling is shown in Fig.2: both groups have overlapped following some joint dependence  $d(\delta F)$ .

The first surprise was in that one of the Lyapunov exponents proved to be nearly constant in the whole range of the empirical data:  $\Lambda_3 \approx -1.25$ . Even though the origin of this peculiarity is not known it allows us to relate both empirical dependences in Fig.2. Besides, we did use this result as an additional check of the computation accuracy.

Indeed, using Eqs.(1.3), (2.4), and (2.5a) we obtain a simple relation

$$\Lambda_1 = \begin{cases} -\Lambda_3(d-2), & d \leq 3 \\ -\Lambda_3 - \Lambda_\Gamma \frac{d-3}{4-d}, & d \geq 3 \end{cases} \quad (3.2)$$

with constant parameters  $\Lambda_3 \approx -1.25$  and  $\Lambda_\Gamma = -2.5$  whatever the dependence  $d(\delta F)$ .

The next, and the main, result was a very slow dependence on  $F$  of all the dimensionless characteristics of chaotic attractors (see Figs.1 and 2). This is why we make use of a logarithmic argument  $F_L = \ln(1 + \delta F)$  rather than of  $\delta F$  itself. That slow dependence prevents us from reaching a close vicinity of the upper bound  $d = 4$ , and thus from clarifying an interesting question in Ref. [1]: if the dimension does asymptotically approach this bound or, instead, saturates at some lower value of  $d$  (for farther discussion see next Section). The maximal value actually reached in our numerical experiments was approximately  $d \approx 3.73$  only due to a rapid increase of the computation time as  $d \rightarrow 4$ .

The empirical dependence  $d(F_L)$  (and hence  $\Lambda_1(F_L)$  as well) has been constructed using the data for the two first groups in Fig.1 with known  $F_{cr}$  values. To this end, let us assume, first, that  $d(F_L)$  does reach the upper bound as  $F_L \rightarrow \infty$ . Further, Fig.2 suggests that this dependence is close to linear near  $F_L = 0$ , hence we added the unity under logarithm in  $F_L$ . Finally, we use a simple relation:

$$d(F_L) = 2 + \frac{4 F_L}{F_0 + 2 F_L}, \quad F_L = \ln(1 + \delta F) \quad (3.3)$$

with a single fitting parameter  $F_0$ .

Surprisingly, the simple empirical relation (3.3) fits, with a particular value of the fitting parameter  $F_0 = 8.5$ , not only the points of the first two groups but also, with a reasonable accuracy (especially for  $d$ ), the rest of points with unknown  $F_{cr}$  values set to zero in Fig.2. Notice that deviations of empirical points from a smooth dependence are not due to computation errors, which were carefully checked, but apparently represent some fine structure of chaotic attractors we did not study in the present work (cf. Ref. [1]).

Still, the agreement between empirical data and analytical relation is not yet satisfactory especially for the two rightmost points with the biggest  $F$ .

For improving the agreement we used two methods. First, we tried to fit the unknown  $F_{cr}$  values for the three groups of points around  $F_L = 7$  (see Fig.1 and the Table). Interestingly, the two groups seem to belong to the same attractor even though they are separated by a wide gap with limit cycles only. Apparently, this is because of the fixed initial conditions (2.3) which may or may not find themselves within the attractor basin for a particular value of  $F_L$  (see also Ref. [2, 1]). For this reason we cannot directly see the vicinity of chaos border for these three groups of points. Hence, the two new values of  $F_{cr}$  are the fitting parameters unlike the first two.

Table. Characteristics of few-freedom chaotic attractors

attractor's number	$F_{cr}$ chaos border	$F_{cr}/F$	$R(F)$ size	$S(F)$ shape
1	173	1	1.41	0.74
2	190	1	1.43	0.75
2	190	0.32	1.7	0.9
3	1913	0.83	1.9	1.0
4	3038	0.93	2.0	1.1
$F > 4000$	$0.8 F$	0.8	2 - 6.5	1 - 1.6

Beyond the five groups we managed to compute just a few scattered points which prevented the location of other attractors. In this region we used another method based on a simple assumption that each point belongs to a separate attractor whose chaos border is directly related to the position of this point

$$F_{cr}(F) = F_s \cdot F \quad (3.4)$$

where  $F_s$  is a new fitting parameter. This method of a statistical nature is, in a sense, opposite to the first one. The assumption (3.4) is very crude, of course, but it allows us to further improve the agreement with empirical relations (3.2) and (3.3) including the point at  $F_L \approx 15$  but not the last one at the biggest  $F_L \approx 16$ .

Certainly, a couple of these 'abnormal' points is too few for any definite conclusions. Yet, they may, and apparently do as we shall see below, indicate a different asymptotic behavior, as  $F \rightarrow \infty$ , compared to the simple relations (3.2) and (3.3). To clarify this important question we turned to the very limit  $F = \infty$ . To reach this limit we may fix parameters  $f$  and  $\mu$ , and set  $\gamma = \omega_2 = 0$  (see scaling (2.1) and (2.2)). In this way we arrive at a conservative system with the simple Hermitian Hamiltonian:

$$H_0(a_1, a_2) = \mu a_1^2 a_2^* + f a_1^* + \text{c.c.} = 0 \quad (3.5)$$

where the latter equality is due to the initial conditions (2.3).

A few sample runs of this limit system revealed that all characteristics (2.5) but the dimension  $d$  of an energy surface now, which is the limit of a chaotic attractor for a finite  $\gamma$ , kept growing with time. This suggests an unbounded motion along some non-compact energy surface, and moreover with the ever increasing dimensional Lyapunov exponent  $\lambda_1 \rightarrow \infty$  for  $t \rightarrow \infty$ .

As to the dimension of the energy surface itself it quickly converges to the maximal value  $d = 4$ . At the first glance, it appears strange as one would

expect this surface to be three-dimensional. The explanation of the apparent paradox is the following. The metric of the motion  $M = (+, 0, 0, -)$  has now two zero Lyapunov exponents: one corresponds to the eigenvector along a trajectory, as usual, while the other one is associated with the eigenvector across the energy surface (the so-called marginal instability, see, e.g., Ref. [6]). It means that this metric characterizes an infinitely narrow four-dimensional layer around the energy surface rather than the surface itself. Notice that the invariant measure of ergodic motion (the so-called microcanonical distribution) on energy surface is determined by the phase-space volume in that layer, and not by area on the surface.

Increasing  $\lambda_1$  in the limit (3.5) is at variance with the asymptotics of Eq.(3.2) for  $\gamma \rightarrow 0$ . Indeed

$$\lambda_1 = \Lambda_1 \gamma \rightarrow \frac{|\Lambda_\Gamma|}{F_0} \cdot \gamma \ln \left( \frac{F_s \mu f}{\gamma^2} \right) \rightarrow 0, \quad \gamma \rightarrow 0 \quad (3.6)$$

To cope with this difficulty we need a power-law argument in the right-hand side of Eq.(3.3) rather than a logarithmic one,  $F_L$ . To this end, we simply added to the latter a power-law term in the form

$$F_L \rightarrow F_L + \exp(\beta(F_L - F_1)) \quad (3.7)$$

with two parameters,  $\beta$  and  $F_1$ . The latter characterizes the crossover to the asymptotic behavior where the Lyapunov exponent is described by the relation

$$\lambda_1 \rightarrow \frac{|\Lambda_\Gamma|}{F_0} \cdot e^{-\beta F_1} \frac{(F_s \mu f)^\beta}{\gamma^{2\beta-1}} \quad (3.8)$$

The limit behavior in system (3.5) ( $\lambda_1$  growth) implies  $\beta > 1/2$ .

There is an interesting possibility to calculate more accurate value of  $\beta$  using our preliminary empirical data for the limit (3.5). The point is that conservative system (3.5) possesses only one quantity of the frequency dimension, the inverse time. So, one may conjecture that the variable  $1/t$  plays in conservative system (3.5) a role similar to that of  $\gamma$  in our main dissipative model (1.1). According to our preliminary data all the motion characteristics (2.5) but  $d$  in the former case are growing with time as a power law. Particularly,  $\lambda_1 \propto t^{1/3}$ . By comparison with Eq.(3.8) we obtain  $\beta = 2/3$  to be used below.

With all these improvements we show in Fig.3 our final (so far!) fitting the empirical data for the attractor dimension and Lyapunov exponents.

The most interesting result of our studies is finding eventually the two quite different chaotic structures with respect to their dependence on the

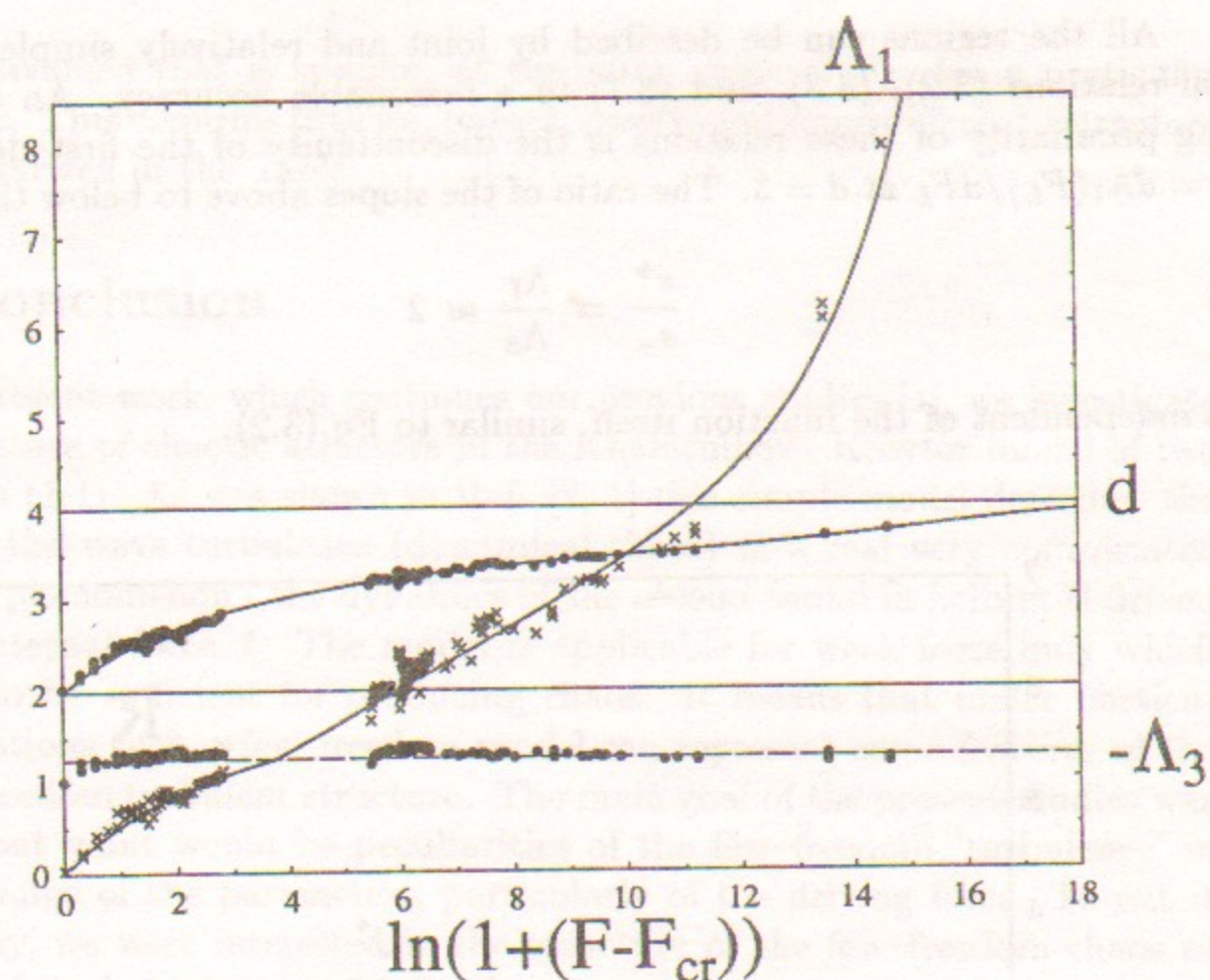


Figure 3: Same as in Fig.2 with two more identified attractors (see the Table), and the statistical estimate (3.4) for the rest. Two curves are old empirical relations (3.3) and (3.2) with a new term (3.7) and fitting parameters:  $F_s = 0.8$ ,  $F_0 = 7.5$ ,  $F_1 = 11.5$ .

principal parameter  $F$ . The most of our empirical data belong to the structure with the slow, logarithmic, dependence. It comprises the region from  $\delta F = (\delta F)_1 \sim 1$  up to the crossover

$$(\delta F)_2 \approx e^{F_1} \approx 10^5 \quad (3.9)$$

Beyond  $(\delta F)_2$  the chaotic structure becomes 'turbulent' with a relatively fast, power-law, dependence on  $F$ . The crossover between the two regions is clearly seen in Fig.3 on the  $\Lambda_1(F_L)$  dependence, and can be noticed in  $d(F_L)$  variation as well. So far, we have no explanation as to a large value of this crossover. However, notice that in the logarithmic scale  $F_L$  the crossover  $(F_L)_2 \approx F_1 \sim 10$  is not that big.

Since the logarithmic dependence in Eq.(3.3) becomes linear for small  $\delta F$  there is actually the third region bounded from above by one more crossover  $(\delta F)_1 \sim 1$ . This region of threshold chaos is most clearly seen in Fig.1.

All the regions can be described by joint and relatively simple empirical relations (3.2), (3.3), and (3.7) to a reasonable accuracy. An interesting peculiarity of these relations is the discontinuity of the first derivative  $s = d\Lambda_1(F_L)/dF_L$  at  $d = 3$ . The ratio of the slopes above to below this point

$$\frac{s^+}{s^-} = \frac{\Lambda_\Gamma}{\Lambda_3} \approx 2 \quad (3.10)$$

is independent of the function itself, similar to Eq.(3.2).

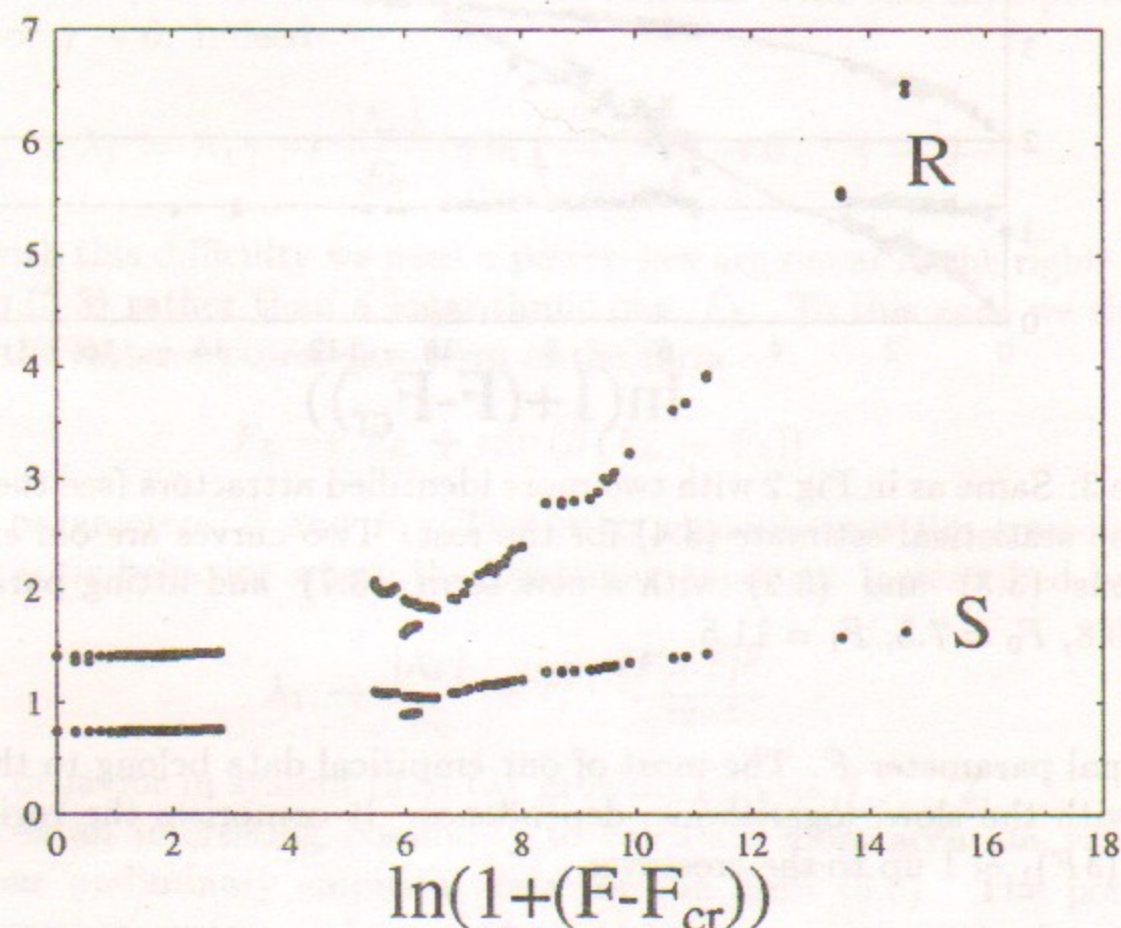


Figure 4: Same as in Fig.3 for the size  $R$  (2.5c) (upper points) and shape  $S$  (2.5d) (lower points).

Finally, we display in Fig.4 the behavior of two geometrical characteristics of chaotic attractor, the size  $R$  (2.5c) and shape  $S$  (2.5d). We did not attempt to construct the empirical relations for these characteristics. However, a clear qualitative behavior of those is also interesting and important. First, both  $R$  and  $S$  grow with  $F_L$  which is also in agreement with the limit behavior in system (3.5). In other words, the attractor becomes more and more large and elongated. Another interesting point is in that the geometrical characteristics

are multivalued that is specific, at the same value of  $F_L$ , for a particular attractor. This confirms that we, indeed, have found some different attractors as summarized in the Table.

## 4 Conclusion

In the present work, which continues our previous studies [1], we investigate the structure of chaotic attractors in the Khalatnikov - Kroyter model of two freedoms (1.1). As was shown in Ref. [2, 1] this simple model describes the birth of the wave turbulence (dynamical chaos) in a real very complicated physical phenomenon - the dynamics of the second sound in helium II driven by an external force  $f$ . The model is applicable for weak force only which proved to be sufficient for producing chaos. It means that under particular conditions such a few-freedom model can represent some features of the many-freedom turbulent structure. The main goal of the present studies was to find out what would be peculiarities of the few-freedom 'turbulence' in a wide range of the parameters, particularly of the driving force. To put it other way, we were interested in the structure of the few-freedom chaos as compared to that of the multi-freedom one.

To this end, we have chosen a number of dimensionless characteristics of the chaotic structure (2.5), and studied their dependence on a single dimensionless parameter  $F$  (2.1) in a series of numerical experiments. We had expected some qualitative differences between the few- and multi-freedom chaos, yet the surprise was in the nature of the difference which proved to be the dependence of chaos characteristics on the principal parameter  $F$ . While in the multi-freedom chaos this dependence is fast (a power law) in a few-freedom chaos it is very slow (logarithmic). Even though our studies were restricted to a particular model we conjecture that this principal difference is of a generic nature. Apparently, it is related to the strict limitation of the attractor dimension in a few-freedom system (to the interval  $2 < d < 4$  in our model).

In spite of satisfaction with this finding we went on in numerical experiments trying to reach as large  $F$  as possible in a reasonable computation time (days), and it was not in vain! First, we tried to find some indication, if any, of deviations from the original empirical relations which could be interpreted as a lower asymptotic dimension ( $d < 4$ ) than assumed above ( $d = 4$ ). Eventually, we have found the deviation but of the opposite sign (see Fig.1 and 3)! Even though this is just two points we put forward a different explanation - the transition to a new, power law, dependence of the attractor

characteristics which is similar to that in a multi-freedom system (Section 3).

Currently, we distinguish, all together, the three regions in the principal parameter  $F$ . In terms of  $\Lambda_1$  they are as follows (see Figs.1 and 3, and Eqs.(3.2),(3.3),(3.7), and(3.9)):

(i) the threshold domain

$$\Lambda_1 = -\Lambda_3(d-2) \approx \frac{4|\Lambda_3|}{F_0} \cdot (F - F_{cr}), \quad F_{cr} < F \lesssim F_{cr} + 1 \quad (4.1a)$$

with a 'turbulent' behavior (cf. Ref. [1]);

(ii) the logarithmic region

$$F_{cr} + 1 \lesssim F \lesssim (\delta F)_2 \approx 10^5 \quad (4.1b)$$

this is our main result revealing a qualitative difference between the few- and multi-freedom chaos, and

(iii) the asymptotics

$$\Lambda_1 \approx \frac{|\Lambda_\Gamma|}{F_0} \cdot e^{-2F_1/3} \cdot F^{2/3}, \quad F \approx \delta F \gtrsim (\delta F)_2 \quad (4.1c)$$

where the dynamics is similar again to a multi-freedom chaos ('turbulence', cf. the first region (4.1a)) provided unbounded motion in the conservative limit (3.5).

Remarkably, all the three regions can be described by a joint empirical relation which is rather simple and reasonably accurate. Particularly, this confirms the assumption that (rather than answer to the question if) the dimension of chaotic attractor in the model considered does reach the upper bound  $d = 4$  (see Eq.(3.3) and above). However, an important question how universal the described structure of the few-freedom chaos might be remains open and certainly deserves further studies. In particular, the above mentioned condition for a power-law asymptotics (unbounded motion in conservative limit (3.5)) is hardly generic. Rather, it is characteristic for a more narrow class of nonlinear models as compared to those with the wide logarithmic region.

## References

- [1] *B.V. Chirikov and V.G. Davidovsky*. Dynamics of a Simple Model for Turbulence of the Second Sound in Helium II, preprint BINP 99-70, Novosibirsk, 1999.
- [2] *I.M. Khalatnikov and M. Kroyter*. Zh. Eksp. Teor. Fiz., **115**, 1137 (1999).
- [3] *D. Farmer, E. Ott and J. Yorke*. Physica D **7**, 153 (1983).
- [4] *D. Farmer*. Physica D, **4**, 366 (1982).
- [5] *A. Lichtenberg and M. Lieberman* Regular and Chaotic Dynamics, Springer (1992).
- [6] *G. Casati, B.V. Chirikov and J. Ford*. Phys. Lett. A, **77**, 91 (1980).



*B.V. Chirikov and V.G. Davidovsky*

**The structure of chaotic attractor  
in a few-freedom dynamical system**

*В.Г. Давидовский, Б.В. Чириков*

**Структура хаотического аттрактора  
в маломерной динамической системе**

Budker INP 99-96

Ответственный за выпуск А.М. Кудрявцев

Работа поступила 18.10.1999 г.

---

Сдано в набор 20.10.1999 г.

Подписано в печать 22.10.1999 г.

Формат бумаги 60×90 1/16 Объем 0.7 печ.л., 0.6 уч.-изд.л.

Тираж 120 экз. Бесплатно. Заказ № 96

---

Обработано на IBM PC и отпечатано на  
ротапринте ИЯФ им. Г.И. Будкера СО РАН

Новосибирск, 630090, пр. академика Лаврентьева, 11.